Materials Letters 199 (2017) 50–52

Contents lists available at ScienceDirect

Materials Letters

journal homepage: www.elsevier.com/locate/mlblue

The air and thermal stabilities of lead-free perovskite variant Cs_2SnI_6 powder

Yanan Jiang, Hailiang Zhang, Xiaofeng Qiu, Bingqiang Cao *

Materials Research Centre for Energy and Photoelectrochemical Conversion, School of Material Science and Engineering University of Jinan, Jinan 250022, Shandong, China

ARTICLE INFO

Article history:
Received 26 February 2017
Received in revised form 10 April 2017
Accepted 10 April 2017
Available online 12 April 2017

Keywords:
Cs_2SnI_6
Perovskite variant
Air and thermal stability
Semiconductor
Solar energy material

ABSTRACT

Cs_2SnI_6, as an inorganic lead-free perovskite variant, is regarded as a more environment friendly photovoltaic material than methylammonium lead iodide perovskite. However, its air and thermal stabilities still remain unclear. In this paper, Cs_2SnI_6 powders were synthesized via a chemical bath deposition method. The crystalline phases, morphologies, and vibrational properties were investigated. Moreover, its phase and morphology can retain in air with high relative humidity over a week even a month. The thermal stability measurements indicate Cs_2SnI_6 is stable up to 270 °C and then decomposes to CsI and SnI_4. These results should pave the way for further application of Cs_2SnI_6 for more stable solar cells.

1. Introduction

Recently, the power conversion efficiency (PCE) of typical hybrid organic-inorganic perovskite $CH_3NH_3PbI_3$ solar cell is over 20% [1]. Considering the toxicity issue of lead (Pb), the tin (Sn)-based hybrid organic-inorganic perovskites ($CH_3NH_3SnX_3$, X = Cl, Br, I) are also of great interest as well, and some tentatively studies have been carried out. For example, Kanatzidis et al.[2] developed a low-temperature vapor-assisted solution method to prepare $CH_3NH_3SnI_3$ films and obtained typical device efficiency of only 1.86%. Snaith et al. [3] reported that the $CH_3NH_3SnI_3$ perovskite solar cell with mesoporous TiO_2 scaffold exhibited PCE of over 6%. But, the photovoltaic efficiency of the Sn-based hybrid perovskite solar cell (PSC) is obviously lower than that of the Pb-based device [3,4]. Moreover, the long-term stability of Sn-based hybrid PSCs remains a greater challenge as $Sn^{(2+)}$ is more easily oxidized and the device deteriorates quickly in moisture [5].

All-inorganic lead-free cesium tin iodide perovskite ($CsSnI_3$) have attracted much attention due to its superior intrinsic physical properties like direct bandgap (~1.3 eV) with its maximum Shockley–Queisser PCE limit of 33% [6,7]. So far, the state-of-the-art PCE of solution-processed $CsSnI_3$ film PSCs without additives is about 3% but all measured in glove boxes [8,9]. Compared with $CsSnI_3$, the cesium tin halide perovskite variant, Cs_2SnI_6 is predicted to be more stable [10,11]. Our group reported the spontaneous oxidation process from unstable $CsSnI_3$ film to Cs_2SnI_6 films in air and found that Cs_2SnI_6 film with a bandgap of 1.48 eV exhibited high absorption coefficient (over 10^5 cm^{-1} from 1.7 eV) [10]. Meanwhile, Cs_2SnI_6 employed as hole transport layer in dye-sensitized solar cell (DSSC) was also reported [11]. But, the stability of Cs_2SnI_6 itself remains unclear and more study is needed.

In this work, we highlight the stability of Cs_2SnI_6 as perovskite variant in air and under heating conditions. The use of tetravalent Sn instead of divalent Pb could simultaneously address the Pb toxicity of $CsPbI_3$ and also enhance the stability of $CsSnI_3$. The air and thermal stabilities are investigated in this study. Our work underscores a new possibility for developing lead-free inorganic perovskite solar cells with high efficiency and pronounced stability.

2. Experimental

Cs_2SnI_6 powder was prepared by a modified chemical bath method [11]. Typically, aqueous HI (6.8 mL, 7.58 M), aqueous H_3PO_2 (1.7 mL, 9.14 M), and deionized water (0.4 mL) were dropped into round-bottom flask and then heating the flask to 120 °C. SnI_2 (372 mg, 1 mmol) and CsI (260 mg, 1 mmol) was added into the hot solution. Then the acetone was added when the powders dissolved. 5 min later, the stirring was discontinued, and left to cool to room temperature. Finally, the precipitates were evaporated to produce dark powders. The material characterization details were presented in Supporting information.

* Corresponding author.
E-mail address: mse_caobq@ujn.edu.cn (B. Cao).

http://dx.doi.org/10.1016/j.matlet.2017.04.046
0167-577X/

3. Results and discussion

The morphology of the as-prepared powders will vary with the increase of the quantity of acetone evidently. A typical octahedral structure as shown in Fig. 1(a) and inset was observed when 7 mL acetone was applied, which shows the average grain size is approximate 7 μm. When the quantity of acetone was up to 10 mL the Cs_2SnI_6 powder shows truncated octahedral with typical grain of about 10 μm as shown in Fig. 1(b). The phase of the Cs_2SnI_6 powder was verified with X-ray diffraction (XRD) measurements, as shown in Fig. 1(c), where the simulated XRD peaks according to PDF file (No. 51-0466) was also presented. The diffraction peaks of the obtained sample match well with the simulated pattern of Cs_2SnI_6, which is a defect variant of the ABX_3-type perovskite structure adopted by the $CsSnI_3$ [11,12]. The Raman spectrum of the Cs_2SnI_6 powder shown in Fig. 1(d) further confirms the perovskite variant structure. There are six typical symmetric stretching vibration modes (ν_1–ν_6) for $[SnI_6]^{2-}$ octahedral in Cs_2SnI_6 [13], among which ν_1, ν_2, and ν_5 modes are Raman-active. Three main peaks in this spectrum at 128.01 cm^{-1}, 91.74 cm^{-1}, and 49.89 cm^{-1} are consistent with ν_1, ν_2, and ν_5 modes, respectively. But the ν_5 mode (49.89 cm^{-1}) at very low wave number is a little different to the pure theoretical prediction (78 cm^{-1}) [14]. The optical absorption property of the as-prepared Cs_2SnI_6 was characterized and the onset of direct absorption feature at near 830 nm was observed, which demonstrated a bandgap of 1.49 eV as shown in Fig. S1, which is well consisted with the bandgap of Cs_2SnI_6 film [10].

Considering the formal tetravalent oxidation state of Sn in Cs_2SnI_6, it is expected to be more stable against oxidation in air. In this study, to check the phase stability, we stored the as-prepared Cs_2SnI_6 powder in moist air with controlled relative humidity of 30–60% and exposed it to natural sunlight illumination for different times. In one week, there is no any impurity XRD peak observed in Fig. 2(a) (red line), indicating that the Cs_2SnI_6 powder is stable. However, a minor CsI impurity peak was observed in the XRD spectrum (Fig. 2(a) blue line) after 30 days. This may imply small partial Cs_2SnI_6 powder decomposed. The simultaneous morphology changes of the Cs_2SnI_6 powder disclosed by SEM observations

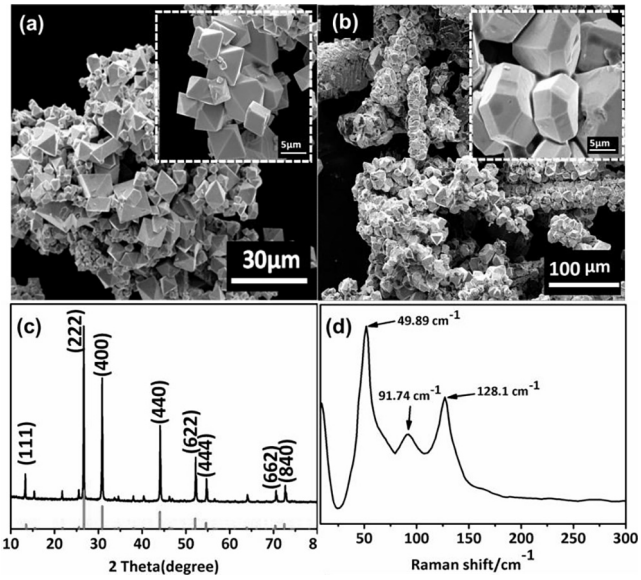

Fig. 1. (a–b) Scanning electron microscope (SEM) images of Cs_2SnI_6 powder synthesised by a chemical bath method using (a) 7 mL, (b) 10 mL acetone and other precursors described in the experimental part. (c–d) The crystalline phase and vibrational property of Cs_2SnI_6 powder, (c) Experimental and simulated XRD patterns and (d) Raman spectrum.

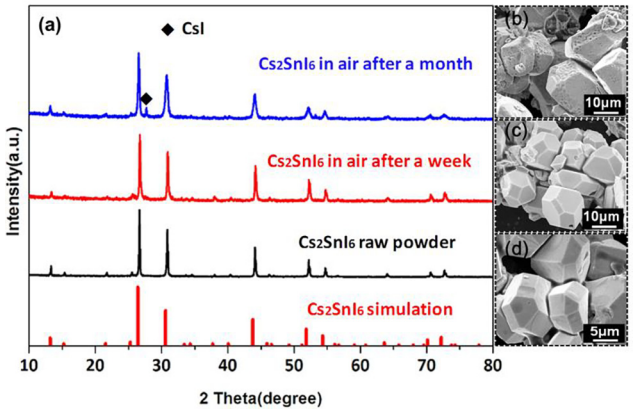

Fig. 2. The air stability of Cs_2SnI_6 powder. (a) XRD patterns of as-prepared Cs_2SnI_6 powder in air after a month, a week, and raw powder. Vertical lines indicate the standard spectra from PDF card (51-0466). Corresponding SEM images of the Cs_2SnI_6 powder in air (b) after a month, (c) after a week, and (d) raw powder.

prove this inference as shown in Fig. 2(b). The well-defined crystallites are almost same in a week but several pinholes appear in crystalline surfaces after a month indicating minor decomposition.

The material thermal stability is also a very important parameter for solar cell application. Fig. 3(a) shows the TGA and DSC curves of the Cs_2SnI_6 powders. About 5% weight lost at near 170 °C (black line) is due to the evaporation of SnI_4 (boiling point

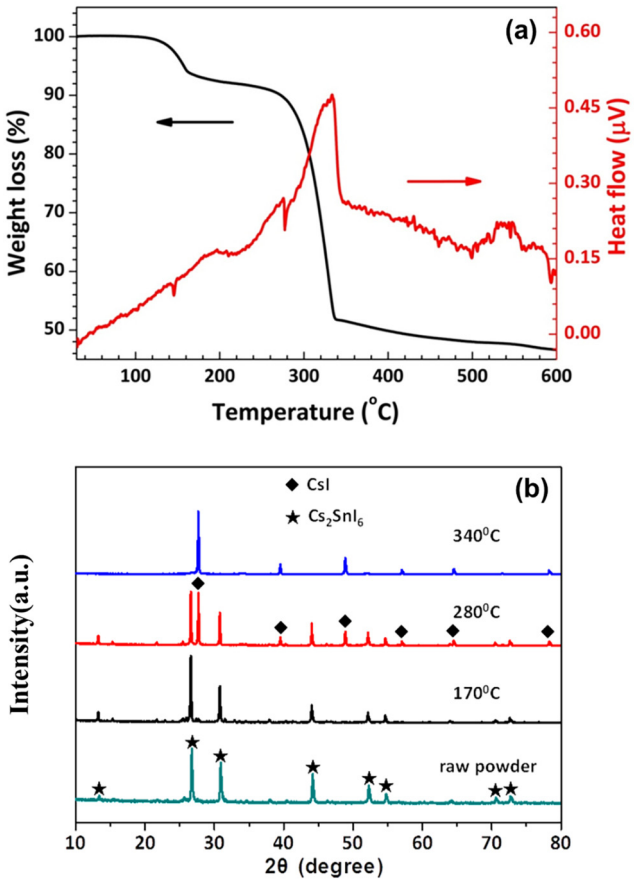

Fig. 3. The thermal stability of Cs_2SnI_6 powder. (a) Differential scanning calorimetry (DSC, red line) and thermogravimetric analyses (TGA, black line) curves of the Cs_2SnI_6 power, (b) XRD patterns after heating at different temperature (170 °C, 280 °C, and 340 °C).

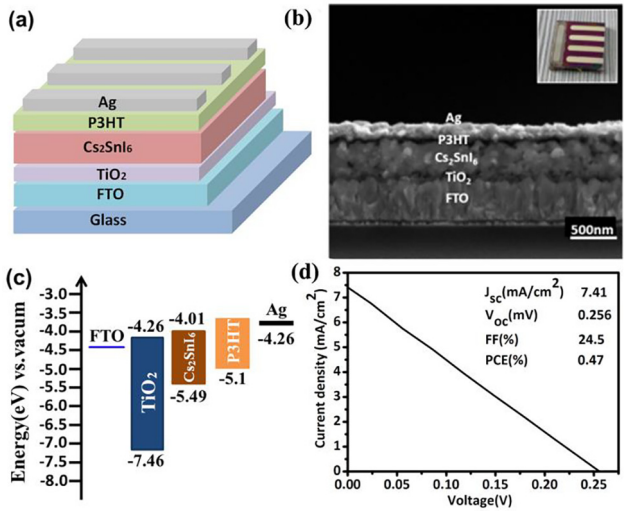

Fig. 4. (a) Schematic structure of FTO/TiO_2/Cs_2SnI_6/P3HT/Ag planar perovskite solar cell device. (b) Cross-sectional SEM image of the complete device and an optical image. (c) Energy band structure of the solar cell. (d) The *J-V* curve of planar perovskite solar cell with Cs_2SnI_6 as light absorber layer.

144 °C), which was oxidized from SnI_2 during the synthesis process [15–17]. The thermal decomposition of Cs_2SnI_6 starts at ~270 °C and the epibiotic white powder still retain ~50% of the initial weight after heating treatment at 340 °C. The XRD pattern shows the decomposition relict is only CsI and the other weight lost is due to the volatile SnI_4. Based on these findings, the chemical reaction involved may as follow:

$$Cs_2SnI_6 \xrightarrow{\Delta} 2CsI + SnI_4 \uparrow,$$

Therefore, Cs_2SnI_6 is more thermally stable than $MAPbI_3$, which decomposes rapidly at 150 °C for 30 min in air [18].

Last, it is worth to note that the more stable Cs_2SnI_6 is already adopted as solar cell absorber [10,19]. We have further exploited it in an N-i-P planar solar cell by utilizing such Cs_2SnI_6 film as the light absorber, and achieved currently a conversion efficiency of 0.47% (shown in Fig. 4). The primary low power conversion efficiency is supposed due to several reasons. First, the phase purity and polycrystalline quality of Cs_2SnI_6 should be further improved. Second, reducing the series resistance and enhancing the shunt resistance by optimizing the electron and hole transporting layers may improve the power conversion efficiency. Last, the innate dynamics of the photoexcited electrons and holes in Cs_2SnI_6 and the fundamental properties of Cs_2SnI_6 like carrier diffusion lengths should be further studied. Our study thus underscores new possibilities for developing lead-free perovskite solar cells with high efficiency and pronounced stability.

4. Conclusion

In conclusion, we have synthesized lead-free inorganic Cs_2SnI_6 through a chemical bath deposition method and its air and thermal stabilities were investigated. The grain morphology and perovskite variant crystal structure of the Cs_2SnI_6 powders were characterized with SEM, XRD, and Raman spectrum. Under natural sunlight irradiation, such Cs_2SnI_6 powder can retain their morphology and phase in air with high relative humidity over a week. Even after one month, only minor decomposition was observed on the crystallite surfaces. Moreover, Cs_2SnI_6 is thermal stable up to 270 °C. All these results indicate Cs_2SnI_6 is more air and thermal stable than its analogous $CsSnI_3$ and $MAPbI_3$, therefore, demonstrate the potential applications in lead-free inorganic perovskite photovoltaic devices.

Acknowledgment

This work was supported by National Natural Science Foundation of China (No. 51472110).

Appendix A. Supplementary data

Supplementary data associated with this article can be found, in the online version, at http://dx.doi.org/10.1016/j.matlet.2017.04.046.

References

[1] W.S. Yang, J.H. Noh, N.J. Jeon, Science 348 (2015) 1234.
[2] T. Yokoyama, D.H. Cao, C.C. Stoumpos, T.B. Song, Y. Sato, S. Aramaki, J. Phys. Chem. Lett. 7 (2016) 76–82.
[3] N.K. Noel, S.D. Stranks, A. Abate, C. Wehrenfennig, S. Guarnera, Energ, Environ. Sci. 7 (2014) 3061–3068.
[4] F. Hao, C.C. Stoumpos, D.H. Cao, R.P.H. Chang, M.G. Kanatzidis, Nat. Photon. 8 (2014) 489–494.
[5] M. Grätzel, Nature Mater. 13 (2014) 38–42.
[6] W. Shockley, H.J. Queisser, J. Appl. Phys. 33 (1961) 510–519.
[7] S. Rühle, Sol. Energy 130 (2016) 139–147.
[8] N. Wang, Y. Zhou, M.-G. Ju, H.F. Garces, T. Ding, S. Pang, X.C. Zeng, N.P. Padture, X.W. Sun, Adv. Energy. Mater. 6 (2016).
[9] K.P. Marshall, M. Walker, R.I. Walton, R.A. Hatton, Nat. Energy 1 (2016) 16178.
[10] X.F. Qiu, B.Q. Cao, S. Yuan, X.F. Chen, Z.W. Qiu, Y.N. Jiang, Q. Ye, H.Q. Wang, H.B. Zeng, J. Liu, M.G. Kanatzidis, Sol. Energy Mater. Sol. C 159 (2017) 227–234.
[11] B. Lee, C.C. Stoumpos, N. Zhou, F. Hao, C. Malliakas, C.Y. Yeh, T.J. Marks, M.G. Kanatzidis, R.P. Chang, J. Am. Chem. Soc. 136 (2014) 15379–15385.
[12] N. Chander, P.S. Chandrasekhar, V.K. Komarala, Rsc Adv. 4 (2014) 55658–55665.
[13] I. Wharf, D.F. Shriver, Inorg. Chem. 4 (1969) 914–925.
[14] K. Nakamoto, Theory and Applications in Inorganic Chemistry, 6th ed., Wiley, New Jersey, 2008.
[15] Y. Sawada, M. Suzuki, Thermochim. Acta 243 (1994) 95–100.
[16] Y. Sawada, M. Suzuki, Thermochim. Acta 254 (1995) 261–266.
[17] V.K. Dwivedi, G. Vijaya Prakash, Solid State Sci. 27 (2017) 60–64.
[18] G.E. Eperon, S.D. Stranks, C. Menelaou, M.B. Johnston, L.M. Herz, H.J. Snaith, Energy Environ. Sci. 7 (2014) 982.
[19] X.F. Qiu, Y.N. Jiang, H.L. Zhang, Z.W. Qiu, S. Yuan, P. Wang, B.Q. Cao, Phys. Status Solidi (RRL) 10 (2016) 587–591.